Domain Growth, Shapes, and Topology in Cationic Lipid Bilayers on Mica by Fluorescence and Atomic Force Microscopy

Ariane E. McKiernan,* Timothy V. Ratto,† and Marjorie L. Longo*
*Department of Chemical Engineering and Material Science, and †Biophysics Graduate Group, Division of Biological Sciences, University of California, Davis, CA 95616

ABSTRACT Domain formation in mica-supported cationic bilayers of dipalmitoyltrimethylammoniumpropane (DPTAP) and dimyristoyltrimethylammoniumpropane (DMTAP), fluorescently doped with an NBD (((7-nitro-2–1, 3-benzoxadiazol-4-yl)-amino)caproyl) phospholipid, was investigated with fluorescence microscopy and atomic force microscopy. Heating above the acyl chain melting temperature and cooling to room temperature resulted in nucleation and growth of domains with distinguishable patterns. Fractal patterns were found for DPTAP, whereas DMTAP domains were elongated and triangular with feathery edges. Reducing the cooling rate or probe concentration for DPTAP bilayers resulted in larger, filled-in domains with more rounded edges. However, for DMTAP, cooling rates mainly affected size and only slightly modified domain morphology. In a saline environment, the domains were dark, and the surrounding continuous region was bright and thus contained the fluorescent probe. However, as the salt concentration was decreased, the dark regions percolated (connected), resulting in bright domains. Atomic force microscopy scans along domain edges revealed that the dark regions in fluorescence images were approximately 1.4 nm thicker than the light regions. Additionally, the dark regions were of bilayer thickness, approximately 4 nm. Comparison of these results in bilayers to well-documented behavior in Langmuir monolayers has revealed many similarities (and some differences) and is therefore useful for understanding our observations and identifying possible growth mechanisms that may occur in domain formation in cell membranes or supported membrane systems.

INTRODUCTION

Two-dimensional domain and island growth in thin organic or inorganic films is of great interest in such fields as microelectronics, optics, and electrochemistry (Barabási and Stanley, 1995). Additionally, two-dimensional domain growth may be involved in many phenomena observed in cell membranes. These phenomena include enhancement in enzyme activity by formation of activator-rich domains (Dibble et al., 1996; Karlsson et al., 1996), membrane budding, and fusion by formation of domains rich in membrane components with certain curvatures (Mukherjee et al., 1999; Verkade and Simons, 1997; Chernomordik et al., 1995), and partitioning of proteins in coexisting phases known as lipid rafts (Rodgers and Rose, 1994; Shenoy-Scaria et al., 1994). Furthermore, passage through a lipid phase transition temperature (for example in cold storage of blood platelets) can induce phase coexistence, resulting in extensive interfacial regions that are suggested to enhance cell leakage (Hays et al., 1996) and inactivate cell functions. Characterizing this phase behavior in actual cell membranes is difficult, however, because of the number and diversity of components and the small dimensions of phase domains.

Domain growth observed during phase coexistence in monolayers of lipids or other organic molecules, spread at an air-water interface, has provided a wealth of information on two-dimensional growth of micron-scale domains. These Langmuir monolayer systems are well defined (e.g., molecular density, ionic conditions, and temperature can easily be varied and measured) and easily characterized (i.e., fluorescence and Brewster angle microscopy can be used to determine domain size, domain shape, and molecular tilt). It has been found that domain characteristics depend on surface density, microstructural properties, the anisotropy of the underlying microstructure, and the kinetics of domain growth in comparison to diffusive processes (Akamatsu and Rondelez, 1992; Möhwald, 1990; Weidemann and Vollhardt, 1996; Moy et al., 1988; Knobler, 1990). Although much has been learned from these studies, there are certain drawbacks to using Langmuir monolayers for studying two-dimensional domain formation. For example, it is difficult to determine if one would observe exactly the same phase behavior in the more biologically relevant bilayer structure. The optical methods used to study monolayers at the air-water interface give little information on sub-micron scale structures. Additionally, a study of monolayer topology requires transfer to solid supports, and it has been shown that rearrangements can occur as a result of transfer (Sikes and Schwartz, 1997; Hollars and Dunn, 1998).

Supported lipid bilayers may serve as an alternative to monolayers for studying basic aspects of two-dimensional domain formation and phase coexistence. These systems have the benefits of being flat over long expanses as in Langmuir monolayers; however, they possess the biologi-

Received for publication 2 November 1999 and in final form 14 August 2000.

Address reprint requests to M. L. Longo, Department of Chemical Engineering and Material Science, University of California, Davis, CA 95616. Tel.: 530-754-6348; Fax: 530-752-1031; E-mail: mllongo@ucdavis.edu.

© 2000 by the Biophysical Society

0006-3495/00/11/2605/11 $2.00

cally relevant lipid bilayer structure. Because these systems are attached to a rigid support, such as mica or silicon oxide, they may be studied by high resolution scanning probe surface analysis techniques such as atomic force microscopy (AFM; Mou et al., 1995; Fang and Yang, 1997; Sikes and Schwartz, 1997; Hollars and Dunn, 1998) and near field scanning optical microscopy (Hollars and Dunn, 1997, 1998; Tamm et al., 1996). If hydrophilic surfaces such as clean glass or freshly cleaved mica are used, the solid support provides a local charge density that acts in concert with surrounding ions to control the density of adsorbed charged species (Sikes et al., 1996; Cremer and Boxer, 1999). This mimics the ionic screening effects that would be encountered by cell membranes in ionic environments. A very relevant example can be found in the formation of simple lipid bilayer structures on charged mineral surfaces which has been hypothesized as one of the essential steps in molecular evolution (for a review, see Trevors, 1997).

Here, we study domain growth and shapes in mica-supported cationic lipid bilayers. We chose cationic lipids because it was shown previously that supported cationic bilayers could be formed by vesicle fusion and scanned by AFM without causing damage to the bilayer (Mou et al., 1995; Fang and Yang, 1997). It was also reported that expanses of >1 micron of defect-free supported bilayer could be formed by heating the supported cationic bilayer above the acyl-chain melting temperature for a short time followed by cooling to room temperature; these defect-free expanses of bilayer were used to condense DNA. We hypothesized that the heating and cooling process used by Mou et al. (1995) resulted in the nucleation and growth of gel phase domains. In order to investigate, we include, in our supported cationic bilayers, a fluorescent NBD lipid probe that partitions into the least-ordered phase when two lipid phases are present (Knobler, 1990). Therefore, domain formation after the heating and cooling step could be studied by fluorescence microscopy. We used fluorescence microscopy to distinguish lipid phases, characterize domain shape and size, and qualitatively assess lipid mobility. We used AFM to characterize bilayer topology. We find that this supported cationic bilayer system displays many similarities in phase behavior in comparison to Langmuir monolayer systems. For example, we observe the presence of coexisting lipid phases (one phase less ordered than the other phase) and unstable domain growth that results in patterns such as fractals. We also observe significant difference in comparison to Langmuir monolayer systems. For example, we find pattern formation in both phases (a phenomena not observed in Langmuir monolayers), growth patterns that depend on acyl chain length in an unexpected way, and the superposition of phase behavior in both monolayers within the domains, a phenomena that is not observed in Langmuir Schaefer deposited bilayers (Hollars and Dunn, 1998).

MATERIALS AND METHODS

Lipids and lipid vesicles

The cationic lipids, DPTAP, DMTAP, DOTAP (dioleoyltrimethylammoniumpropane), and fluorescent lipid NBD-PC ((1-palmitoyl-2-[-6[{7-nitro-2–1, 3-benzoxadiazol-4-yl}amino]caproyl]-sn-glycero-3-phosphatidylcholine)), one C16 acyl chain, and one C6-N-NBD acyl chain, were purchased from Avanti Polar Lipids, Inc. (Alabaster, AL) and stored in chloroform. All lipids were used without further purification. Small unilamellar vesicles were formed by tip sonication (Branson sonifier, Model 250, Branson Ultrasonics, Danbury, CT) of a 0.5 mg/ml lipid suspension in a saline solution or purified water (the method of resuspension and sonication is the same as described in McKiernan et al. (1997), except that we used two 30-s ultrasonic bursts). Vesicles either contained 2, 3, 5, or 0 mole % NBD-PC. All water used in these experiments was purified in a Barnstead Nanopure System (Barnstead Thermolyne, Dubuque, IA) (resistivity μ 17.9 MΩ, pH $\sim$5.5).

Cationic lipid layer formation on mica and glass substrates for fluorescence imaging

A freshly cleaved mica disk (Muscavite, Pelco, Ted Pella, Inc., Redding, CA) 25 mm in diameter or a pre-cleaned glass slide 25 mm in diameter (Fisher Scientific, Pittsburgh, PA), a polytetrafluoroethylene spacer, a rectangular glass coverslip, and an aluminum platform were used to form an assembly suitable for fluorescence microscopy viewing. The assembly and bilayer formation procedure is described in detail in McKiernan et al. (1997). The assembly was filled with a sonicated cationic lipid vesicle solution and incubated at room temperature for 30 min in a small aluminum and glass chamber humidified by drops of water (see McKiernan et al., 1997, for detailed description). The assembly was then heated to 70°C for 30 min in a laboratory oven. Cooling was accomplished either by turning off the oven and allowing it to cool to room temperature, which required several hours, or by moving the sample to a room temperature environment, which required $\sim$30 min. To eliminate unfused lipid vesicles, the internal contents of the assembly were then rinsed with approximately 10 internal volumes of the solution used to suspend the vesicles. The mica- or glass-supported membrane remained hydrated at all times during this preparation and subsequent fluorescence microscopy.

The cooling rates corresponding to oven-cooling or room-cooling conditions were determined at temperatures near the phase transitions of the lipid + NBD-PC bilayers (see below for phase transition determination). This was accomplished by clamping a flat resistive temperature device temperature sensor (described below) to the mica while cooling was taking place and reading temperatures from the controller described below. It was determined that the oven-cooling rate was approximately 0.2°C/min and the room-cooling occurred at approximately 2°C/min.

Membranes that were used to study domain formation upon heating from room temperature were treated as follows. Sonicated lipid vesicles in 20 mM NaCl were incubated on the mica substrate in the assembly described above at room temperature for 90 min (the chamber described above provided a humid environment). The assembly was then flushed 10 times with room temperature 20 mM NaCl solution. Subsequently, the assembly and its humidified chamber were placed inside a hollow plastic box to provide an environment suitable for heating. A hole in the bottom of the box allowed fluorescence microscopy imaging of the mica or glass surfaces in the assembly. A Thermofoil heater (model HK5485R21.9L12A, Minco Products, Inc., Minneapolis, MN) was used to heat the sample by placing it inside the box on top of the aluminum chamber. The temperature was read using a RTD temperature sensor (model S651PDY24A, Minco Products, Inc., Minneapolis, MN) that was clamped to the top of the mica disk. The temperature was displayed and controlled by a miniature autotune temperature controller (model CN9111A, Omega Engineering, Inc., Stamford, CT).

Fluorescence microscopy

The supported membranes were viewed using a Nikon Diaphot 300 inverted fluorescence microscope (Nikon, Inc., Melville, NY) with a 20×, 40×, or 60× Nikon objective and illuminated by a mercury or xenon lamp using a filter that allowed maximum excitation at 488 nm. Images of the membranes were taken with either a Nikon FE2 35 mm camera or a digital camera (Optronics, Inc., Goleta, CA). Images in Fig. 4, *A* and *B*, were taken using a confocal fluorescence microscope (LSM 410, Carl Zeiss, Inc., Thornwood, NY) and 488 nm excitation from an argon laser (Spectra Physics, Mountain View, CA). The confocal microscope was fitted with a temperature-controlled environmental chamber. Qualitative fluorescence recovery after photobleaching (FRAP) experiments were performed to detect probe mobility within the cationic membranes as follows. A 60× or 40× Nikon objective was used to photobleach an area in the membrane while closing down the field diaphragm of the microscope to its minimum size. Photobleaching was performed for 2 min with subsequent viewing with either a 40× or 20× objective, respectively, and neutral density filters to prevent further bleaching during viewing. Digital camera images of the bleached spots were taken over time and compared to the original bleached spot immediately after photobleaching. If the spot remained after 20 min, the membrane was determined to be immobile, whereas if there was no evidence of a spot remaining after 20 min, the membrane was determined to be mobile. Qualitative FRAP was also performed with the confocal microscope using virtually the same technique.

AFM sample preparation and imaging

For all AFM work, an 80-μl drop of lipid vesicle solution in 20 mM NaCl was placed on the surface of a freshly cleaved mica disk and allowed to incubate at room temperature in a petri dish containing drops of water for 30 min. If a heating and cooling cycle was applied, the sample was heated to 70°C for 30 min in an oven or a water bath. The sample was then cooled by moving it to a room temperature environment and, after cooling, rinsed 10 times with 20 mM NaCl. When no heat was applied (as in the case of the sample in Fig. 8), the mica was simply rinsed with 20 mM NaCl after 90 min of room temperature incubation with lipid vesicles. Finally, samples were usually stored overnight in the refrigerator before AFM imaging (we noted no difference in sample topology or appearance with or without refrigeration). Samples were imaged the following day with a Digital Instruments NanoScope IIIa (Santa Barbara, CA) in force mode with either a J or E scan head. Sharp, coated AFM microlevers, model MSCT-AUHW (Park Scientific, Sunnyvale, CA) were used for all scans. Hydration of the samples during scanning was maintained using Digital Instruments' AFM Tapping Mode Fluid Cell, model MMTFC. All scans were done at room temperature and in contact mode. Set points ranged from 0.25 to 1.0 V with scan rates between 1.5 and 8 Hz. Occasionally, after AFM scanning, we would examine a heat-treated sample by fluorescence microscopy, and we found that the samples looked qualitatively identical to samples that were prepared for fluorescence imaging.

Differential scanning calorimetry (DSC)

DSC was used to determine the phase transition temperatures for DMTAP, DPTAP, DMTAP + 3 mole % NBD-PC, and DPTAP + 3 mole % NBD-PC. Multilamellar vesicle solutions (10 mg/ml) were made up in 20 mM NaCl. These solutions were heated to above 60°C and vortexed to ensure adequate hydration. Samples (150 μl) were scanned in a Calorimetry Sciences Corp. (Spanish Fork, UT) DSC scanner at 1°C/min.

RESULTS

Phase transition temperatures

We observed one transition from gel to liquid crystalline phase in DPTAP + 3% NBD-PC between ~42°C and ~52°C. The transition was centered at 45.4°C. The results using DPTAP containing no NBD-PC were basically the same. Two transitions were found with DMTAP + 3% NBD-PC. One transitions occurred between ~30°C and 34°C and was centered at 31.9°C. A more highly endothermic transition was seen between ~36°C and 44°C and was centered at 38.9°C. The results for DMTAP containing no NBD-PC were basically the same (two transitions were observed).

Domains in DPTAP and DMTAP: shapes and sizes by fluorescence microscopy

Deposition of DPTAP or DMTAP vesicles (containing 3% NBD-PC) on mica followed by heating to 70°C and cooling to room temperature resulted in visible domain formation. The domain shapes seen in these cationic bilayers at room temperature depended on the lipid acyl chain length (C16 for DPTAP and C14 for DMTAP) and solution salt concentration. Fractal-like domains were seen for DPTAP (Fig. 1, *A*, *B*, and *F*, and Fig. 2) compared to elongated triangular domains for DMTAP (Fig. 3, *A* and *B*). Note that domains in which tip-splitting is clearly evident (as observed in the case of DPTAP) are usually referred to as fractal, whereas dendritic domains contain thin straight branches with stable tips (Akamatsu and Rondelez, 1992; Weidemann and Vollhardt, 1996; Knobler, 1990). Membrane domain sizes and shapes did not visibly change over several days at room temperature. Lipid bilayers deposited onto mica from cationic lipid vesicles containing unsaturated acyl chains, DOTAP, were uniformly fluorescent.

DPTAP + 3% NBD-PC bilayers on mica in 20mM NaCl formed dark, fractal domains surrounded by a continuous sea of fluorescence (Fig. 1, *A* and *B*). When the cooling rate used for sample preparation was ~2°C/min, most visible domains at room temperature ranged from ~10 to 50 μm in size (Fig. 1 *A*). When the cooling rate was reduced, ~0.2°C/min, the domain sizes (Fig. 1 *B*) were typically four times larger than those seen for the faster cooling rate. At the slower cooling rates, the domain features took on more of a rounded and filled-in appearance (Fig. 1 *B*). Qualitative FRAP revealed that the bright parts of the membrane were immobile at room temperature (this lipid is in the relatively immobile gel phase at room temperature). In contrast, we found that DOTAP membranes formed on mica were mobile at room temperature (note that DOTAP should be in the liquid phase at room temperature because of its two unsaturated acyl chains).

We investigated the effect that probe concentration plays in determining domain morphology by forming DPTAP

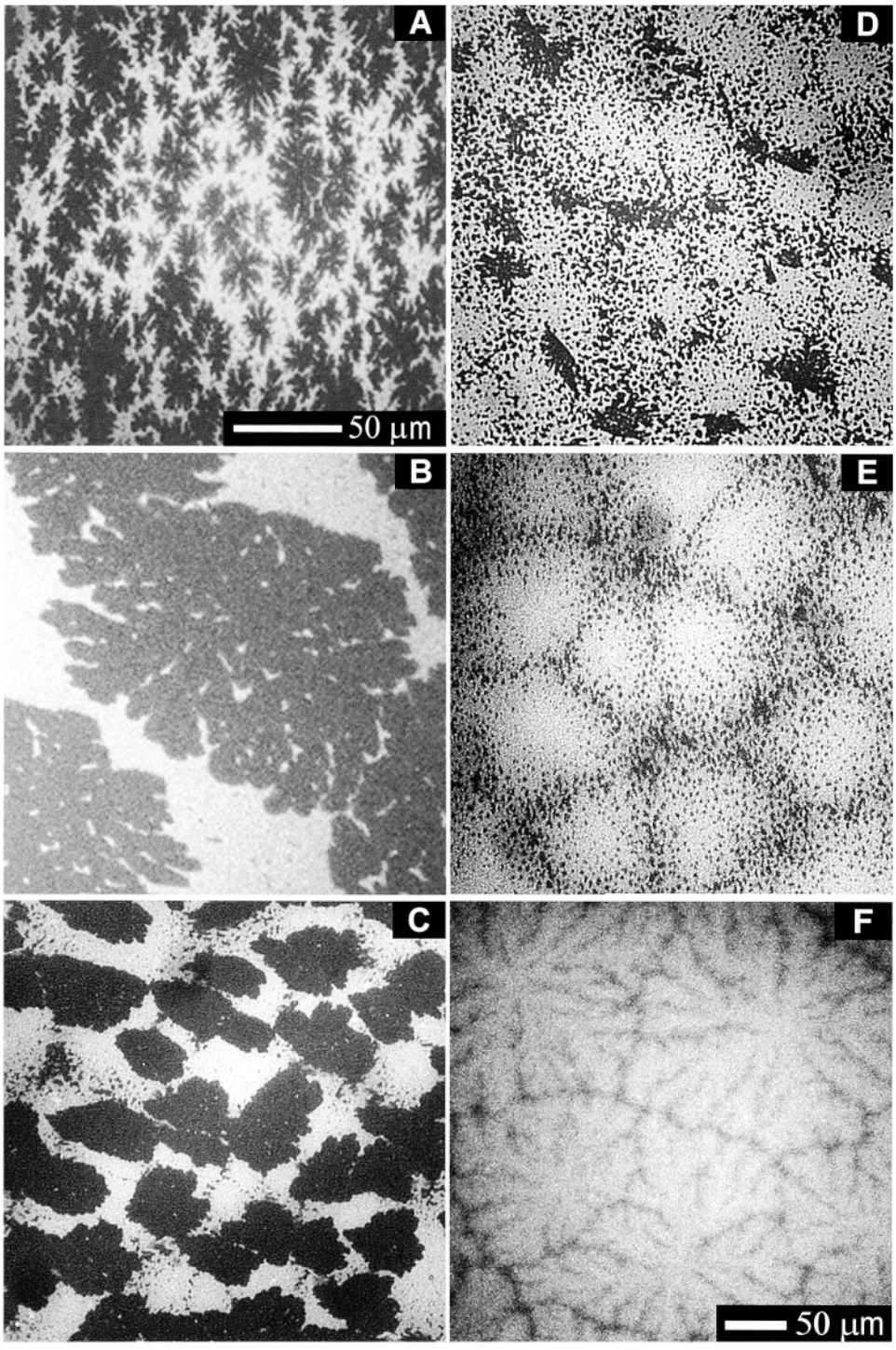

FIGURE 1 Fluorescence microscopy images of mica-supported DPTAP + NBD-PC bilayers showing effect of cooling rate (compare *A* and *B*), probe concentration (compare *A* and *C*), and NaCl concentration (compare *A*, *D*, *E*, and *F*). Magnification is the same in *A-E*. Supported bilayers were formed by vesicle fusion and then subjected to a heating (to 70°C) and cooling (to room temperature) cycle. (*A*) Cooling rate ~2°C/min, 3% NBD-PC probe, bathing solution 20 mM NaCl. Note that the fractal domains are dark in this image. In comparison to the sample in *A*, the samples in the following images were made with (*B*) lower cooling rate, cooling rate ~0.2°C/min; (*C*) lower probe concentration, 2% NBD-PC; Lower NaCl concentration; (*D*) 15 mM NaCl; (*E*) 5 mM NaCl; and (*F*) 0 mM NaCl. Note that the dark domains have percolated (all connected) between 0 and 5 mM NaCl.

supported bilayers containing 2%, 3%, and 5% NBD-PC probe. Bilayers formed with 2% probe (Fig. 1 *C*) contained dark domains that were more filled in and larger (~25–100 μm) in comparison to domains formed when 3% probe was present (Fig. 1 *A*). Inclusion of 5% probe (image not shown) mainly resulted in a further reduction in size (approximately 5–20 μm) of the domains and similar fractal-like shape in comparison to samples containing 3% probe.

We investigated the effect that ionic screening plays in the observed domain behavior by forming DPTAP + 3% NBD-PC supported bilayers (cooled at a rate of 2°C/min) at 15, 10 (not shown), 5, and 0 mM NaCl (Fig. 1, *D-F*). As the ionic strength was reduced, the dark domains decreased in size and surface coverage and become aligned into a network (see for example, Fig. 1, *D* and *E*). Between 5 and 0 mM NaCl, the dark domains join to form a continuous

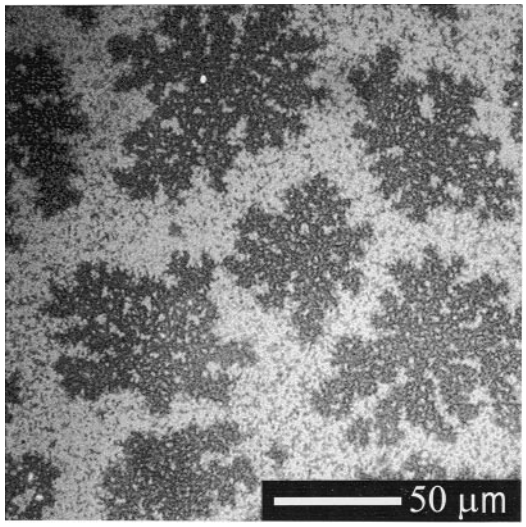

FIGURE 2 Fluorescence microscopy image of glass supported DPTAP + 3% NBD-PC in 15 mM NaCl. Note that the proportion of the surface covered with dark domains is closest to Fig. 1 *A* (20 mM NaCl, mica) and is more than in Fig. 1 *D* (15 mM NaCl, mica) as a result of the higher surface charge of glass in comparison to mica.

network that surrounds large bright fractal domains (Fig. 1 *F*). Thus, by decreasing the salt concentration, the continuous lipid regions are exchanged from bright to dark. The exact condition (in this case, NaCl concentration) in which such an exchange occurs is referred to as the percolation threshold, where "percolation" describes the connectivity of one phase in the presence of a coexisting phase (Vaz, 1995). Thus, the percolation threshold occurs between 0 and 5 mM of NaCl.

Deposition of DPTAP vesicles (containing 3% NBD-PC) on glass followed by heating to 70°C and cooling to room temperature resulted in the formation of domains with similar fractal-like shapes in comparison to domains formed on mica. However, under the same ionic conditions, more of the glass surface was visibly covered with dark domains in comparison to mica surfaces. To demonstrate this, we show a DPTAP sample on glass formed in 15 mM NaCl (Fig. 2). This sample compares most closely to the 20 mM NaCl sample on mica (Fig. 1 *A*) in regard to surface coverage. Additionally, the fractal-like domains are larger on glass substrates in comparison to mica substrates.

DMTAP + 3% NBD-PC domains were elongated and feathery. Using a cooling rate of ~2°C/min during sample preparation, large elongated triangular domains that are about 100 μm in length can be observed at room temperature. These domains are oriented in roughly the same direction and are often connected to neighboring domains (Fig. 3 *Ai*). The regions between the triangular domains contain a high concentration of much smaller dark elongated domains (Fig. 3 *A*, *i* and *ii*). Closer inspection (Fig. 3 *Aii*) revealed that the larger domains are formed by the close alignment of many of the smaller elongated domains, giving the wider

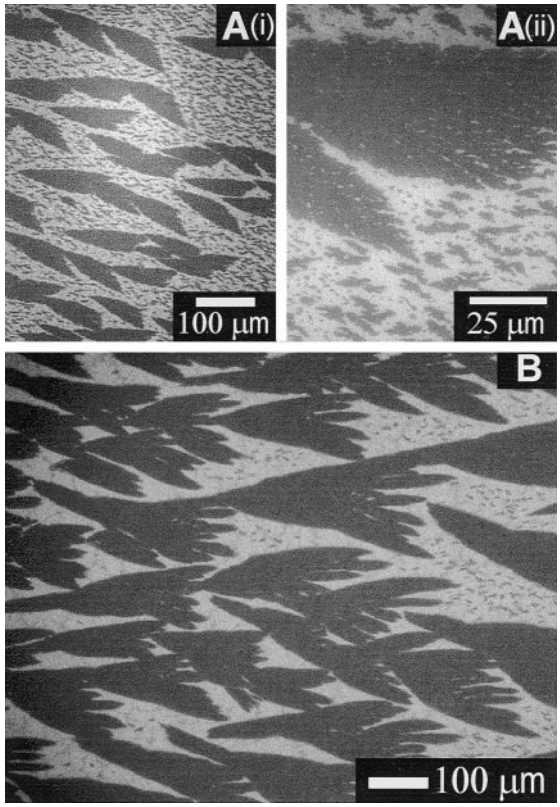

FIGURE 3 Fluorescence microscopy images of mica-supported DMTAP + 3% NBD-PC bilayers in 20 mM NaCl that were subjected to heating and cooling cycle. Domains are elongated and triangular shaped with a feathery texture. A high density of small elongated domains can be seen in the region between the large domains. (*A*) Cooling rate ~ 2°C/min. (*i*) Triangular shaped domains. (*ii*) Higher magnification image shows that domains have feathery texture. (*B*) Cooling rate ~0.2°C/min.

end ("tail") of the triangles a feathery appearance and the other edges a fairly straight (or slightly curved) appearance. A slower cooling rate (~0.2°C/min) produced larger domains (Fig. 3 *B*) (hundreds of microns) but with the same basic shape observed with a reduced cooling rate. We have named this the "flying ducks" pattern. It should be noted that the dark pattern is approximately mirrored in the light pattern due to the symmetry of the pattern. Qualitative FRAP revealed that the bright regions of these DMTAP samples were not mobile at room temperature.

Observations of domain formation

To determine if visible domains existed before any heating of samples, we deposited DPTAP + 3% NBD-PC vesicles in 20 mM NaCl on mica as we did for the samples discussed above, and then rinsed out any unbound lipid. In this case, no heating or cooling was performed. We observed that the fluorescence in the membrane was fairly uniform except for a barely distinguishable mottled appearance (Fig. 4 *A*). Heating of the membrane on the microscope stage resulted

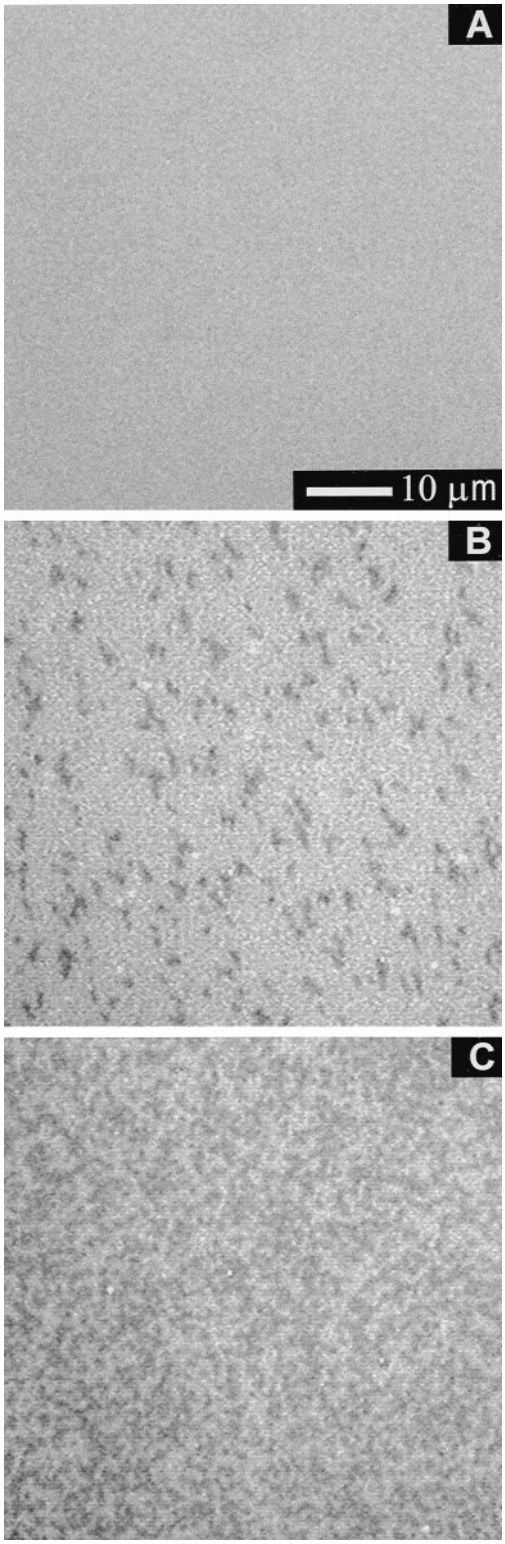

FIGURE 4 Fluorescence microscopy images of mica-supported DPTAP + 3% NBD-PC bilayer in 20 mM NaCl. Magnification is the same in all images. Supported bilayer was formed by vesicle fusion (no heating and cooling cycle) and then was imaged at (*A*) room temperature, (*B*) 42°C, and (*C*) 46°C. Note that the phase transition begins at ~42°C. Brightness was adjusted in these images so that the light regions are of approximately the same brightness in all three images.

in the appearance of small (several micron) dark domains in the bilayer just above 40°C (Fig. 4 *B* was taken at 42°C). The distances between dark domains appeared to range from 2.5 to 10 μm; as more domains appeared in the membrane with increasing temperature, domains were <1 μm apart (Fig. 4 *C* was taken at 46°C). The membrane on the mica surface was completely featureless, showing uniform fluorescence at approximately 48°C and above. Cooling the sample again resulted in fractal domain growth that began at approximately 44°C.

The effects of other cooling rates can be examined by simply heating a membrane containing domains until the membrane becomes homogeneously fluorescent, and then cooling it at a selected rate. Fig. 5, *A* and *B*, shows domain growth in a DMTAP membrane as the membrane was cooled at a rate of approximately 4°C/min. We observed that domain growth began at ~37°C. Small elongated features are seen to grow more in length than in width and to merge with adjacent growing features (Fig. 5, *A* and *B*). The ultimate domain sizes seen at room temperature (10–25 μm) are approximately one-quarter the size of domains formed at a cooling rate of 2°C/min (Fig. 3 *A*). There are significant similarities between the shapes of these domains and those formed at the slower cooling rates. For example, the larger domains in Fig. 5 *B* often have a triangular shape. We also performed qualitative FRAP on these DMTAP samples both at room temperature and after heating to above the acyl chain melting temperature of the lipid. At room temperature, the bright regions between the dark domains were relatively immobile. However, at a temperature of 50°C, which is above the chain melting temperature, the homogeneously fluorescent sample was mobile.

AFM studies on DPTAP bilayer membranes

AFM can be used to determine height differences (and thus acyl chain tilt differences) between lipid domains and surrounding continuous lipids and layer height (if deep defects exist in the layer). Additionally, subtle features, such as sub-micron sized domains that cannot be seen in an optical microscope, can be observed (Hollars and Dunn, 1998). We scanned a DPTAP + 3% NBD-PC mica-supported membrane in 20 mM NaCl (cooled at ~2°C/min) and observed fractal-like domains (Fig. 6 *A*) that were higher by ~1.4 nm (Fig. 6 *B*) than their surroundings, and thus are seen as bright areas in Fig. 6 *A*. These domains were of similar size and shape to the dark domains seen in our fluorescence images of samples prepared at the same cooling rate (Fig. 1 *A*). Thus, the dark regions in the fluorescence images are thicker by ~1.4 nm than the bright regions. Occasionally, holes of ~4 nm, in depth in comparison to the level of the domains, were found at domain edges.

To further investigate the effect of the NBD-PC probe on domain formation, we scanned samples of DPTAP that contained no probe (Fig. 7 *A*) and had been cooled at

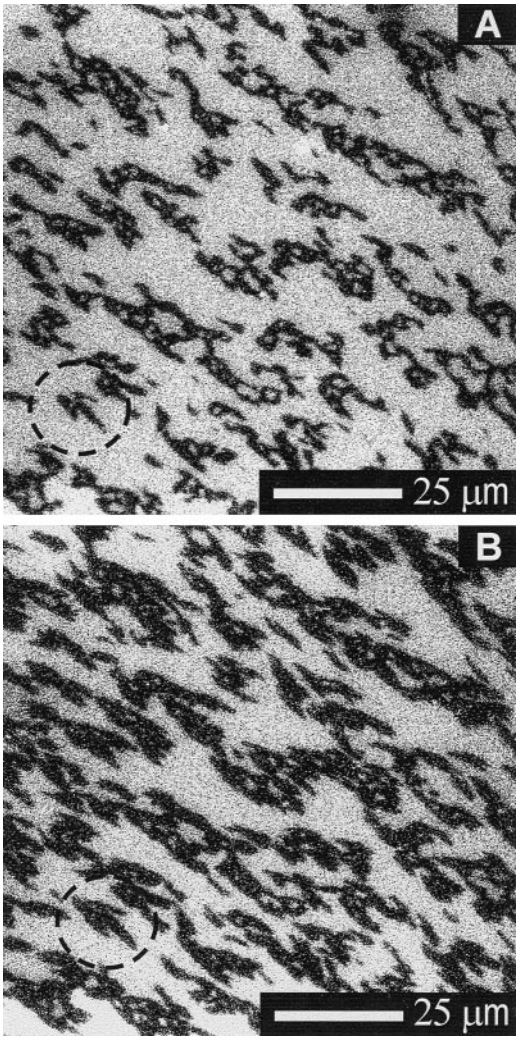

FIGURE 5 Fluorescence microscopy images of mica-supported DMTAP + 3% NBD-PC bilayer in 20 mM NaCl that was subjected to heating and cooling cycle (cooled at ~2°C/min). The membrane was then heated to 50°C (triangular domains as seen in Fig. 3 *A* disappeared and membrane became homogeneously fluorescent) and then cooled to room temperature at ~4°C/min, resulting in domain growth; small aligned domains grow and merge (for example in *A* and *B*, three adjacent domains in the circled area grow into each other). (*A*) 34°C, (*B*) 25°C. Brightness was adjusted in these images so that the light regions are of approximately the same brightness in both images.

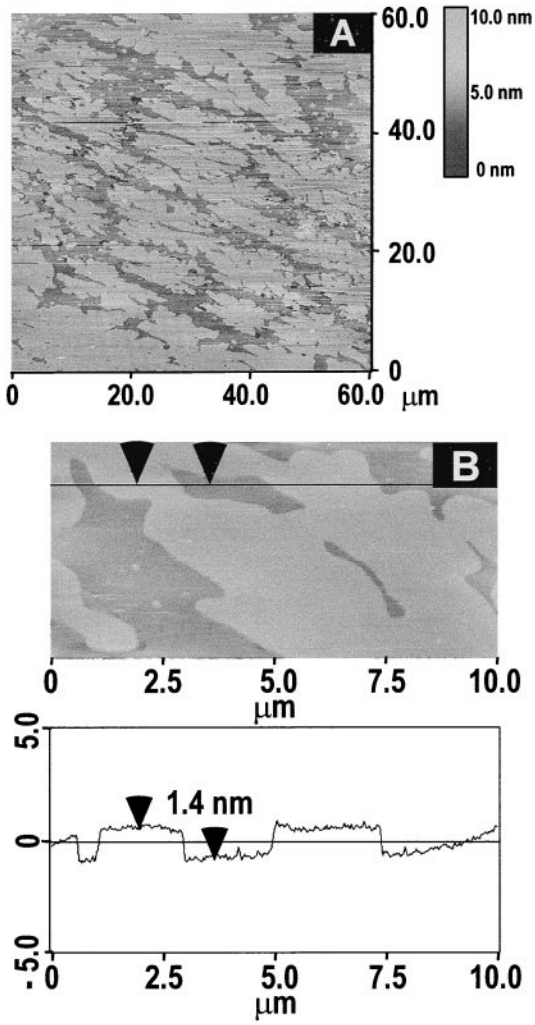

FIGURE 6 AFM images of mica-supported DPTAP + 3% NBD-PC bilayer in 20 mM NaCl that was subjected to heating and cooling cycle (cooled at rate ~ 2°C/min). (*A*) 60 μm × 60 μm scan showing that the fractal domains seen in Fig. 1 *A* are higher than the surrounding continuous region. (*B*) Section demonstrating that domains are ~1.4 nm thicker than surrounding regions. Occasional deep holes adjacent to the fractal domains are ~4 nm deep in comparison to domain height (not shown in this section).

~2°C/min. These surfaces contained a high density of randomly wandering valleys approximately 1 to 20 μm in width. These valleys were either ~1.4 nm or ~4 nm lower than the adjacent level (plateau level). The wider valleys (see top left corner of Fig. 7 *A*) were mainly 1.4 nm lower than the adjacent plateau level and often contained islands and fingers that were of the same height as the plateau level (Fig. 7 *B*). At the center of the island and fingers were craters approximately 4 nm deep, possibly caused by lipid dewetting of the mica surface (Fig. 7 *B*) when the islands were formed. These 4-nm-deep valleys and holes were quite common in samples prepared with no probe, whereas they were only seen rarely in probe-containing samples. Additionally, mounds of lipid material were found in the samples without probe causing the AFM tip to skip across the surface, giving the dark and bright horizontal lines seen in Fig. 7 *A*. Such mounds were rare in probe-containing samples.

Using AFM, we observed micron-scale domains in DPTAP + 3%NBD-PC samples that were never subjected to the heating and cooling cycle (Fig. 8). These domains did not have any distinctive shape or pattern. Recall that domains were not readily visible in the fluorescence images of samples prepared in the same way (discussed above, Fig. 4 *A*) possibly because the domains were too small to

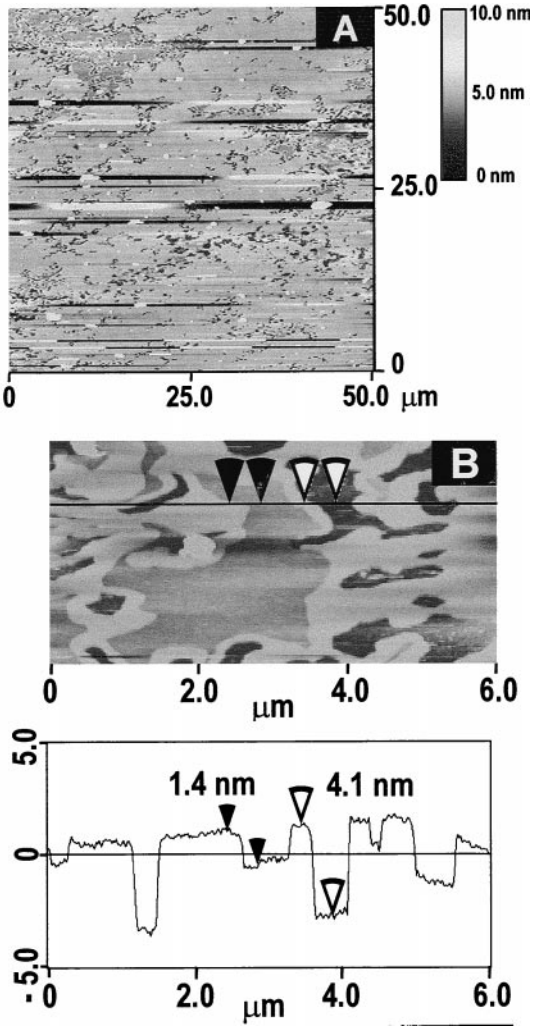

FIGURE 7 AFM images of mica-supported DPTAP bilayer in 20 mM NaCl that was subjected to heating and cooling cycle (cooled at ~2°C/min). Note that this membrane contained no NBD-PC probe. (*A*) No obvious domains are seen. Instead, numerous valleys of two different depths (~1.4 nm and ~4 nm) are carved through the main level "plateau level". Larger valleys of ~1.4 nm depth often contained "plateau level" islands or fingers as can be seen in the top left portion of this image. Formation of these islands and fingers seemed to dewet the surface and ~4 nm deep craters could be observed in the middle of the islands. (*B*) Section from a larger valley shows that the valley is ~1.4 nm deeper than the "plateau level" islands and the interior of the islands contains craters that are ~4 nm deeper than the "plateau level".

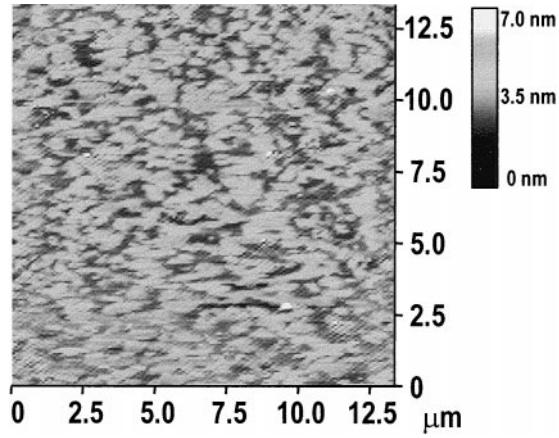

FIGURE 8 AFM images of mica-supported DPTAP + 3% NBD-PC bilayer in 20 mM NaCl. Supported bilayer was formed by vesicle fusion (no heating and cooling cycle) and then was imaged at room temperature. Note that only micron scale domains exist.

resolve with fluorescence microscopy. Furthermore, the presence of micron-scale domains may have resulted in the slightly mottled appearance noted in the fluorescence images.

DISCUSSION

Significance of measured step heights

Occasional holes in the deposited films of DPTAP on mica were found to have depths of ~4 nm. Bilayers of gel phase lipids of similar chain length (e.g., dipalmitoylphosphatidylcholine, DPPC) have been shown by x-ray diffraction to be approximately 4 nm thick (Marsh, 1990). Thus, we believe that the behavior observed here occurred in bilayers of lipids, not in monolayers. We measured a consistent height difference of about 1.4 nm at the domain edges in DPTAP bilayers on mica. These abrupt steps at domain edges occur because of a difference in acyl chain tilt between neighboring phases, as has been previously demonstrated using scanning probe microscopy of supported monolayers (Hollars and Dunn, 1997, 1998; Masai et al., 1996; Yang et al., 1994a,b, 1995). Therefore, bright regions in our fluorescence images are composed of a lipid phase with more tilt with respect to the surface normal, in comparison to the dark regions, which contain a lipid phase that is less tilted. Previous observations show that NBD-PC fluorescent probes prefer to partition into the more disordered phase when two lipid phases coexist (Akamatsu and Rondelez, 1992). Therefore, the more tilted phase is more disordered in comparison to the less tilted phase. We saw no significant fluorescence in the less tilted phase in comparison to the more tilted phase. Thus, it is likely that there is superposition of the phase behavior of opposing monolayers in the less tilted regions. Similar coupling of monolayer phases has been demonstrated recently in giant vesicles containing phase-separated lipid bilayers (Korlach et al., 1999).

Comparison to coexisting phases in monolayers

Ramified morphologies, such as the fractal and feathery textures that we observed for cationic bilayers on mica, are characteristic of an instability in the two-dimensional domain growth process (Barabási and Stanley, 1995). It has been demonstrated previously that very similar domain

shapes (fractal and dendritic) occur in the liquid condensed (LC) phase in Langmuir monolayers when the LE (liquid expanded) phase is compressed or cooled rapidly into the LE-LC phase coexistence regime (Weidemann and Vollhardt, 1995; Akamatsu and Rondelez, 1992). These same fractal or dendritic shapes in LE-LC monolayers can also originate because of the presence of a probe that controls the domain growth process (Knobler, 1990). In both cases, slow diffusion rates of lipid in comparison to domain formation time results in unstable growth of the domain wall. Analogously, we demonstrate here that both the rapid cooling rates and the presence of the NBD-PC probe contribute to the ramified appearance of domains in cationic bilayers.

The presence of fractal patterns in DPTAP (versus, e.g., dendritic patterns) indicates that domain growth is not strongly correlated with crystallographic directions in the gel phase of DPTAP and thus takes place isotropically (Knobler, 1990; Akamatsu and Rondelez, 1992; Weidemann and Vollhardt, 1996). We did not observe any relaxation to rounded structures, even after several days because our lipids are relatively immobile at room temperature (diffusion rates in the gel phase are approximately four orders of magnitude less than in the liquid phase). In contrast, the molecules in fractal or dendritic domains in Langmuir monolayers are more mobile and will relax into more rounded equilibrium structures after several hours (Knobler, 1990; Akamatsu and Rondelez, 1992; Weidemann and Vollhardt, 1996). We did observe rounding in DPTAP if slower cooling rates were used. Similarly, in monolayers, slower compression rates give more rounded LC domains (Weidemann and Vollhardt, 1995).

Surprisingly, we observed very different behavior for bilayers of DMTAP on mica in comparison to DPTAP. DMTAP domains resemble flying ducks. The domains were relatively symmetric about their long axis but unsymmetrical from the "duck's" nose to its feathery tail. Additionally, straight or slightly curved edges existed over relatively long distances (10–100 microns). The observed patterns appear to constitute a new shape of lipid or surfactant domain, since we could not find any similar domain structures in the monolayer literature. The alignment of domains and the high density of small elongated domains may indicate that during growth, there is nematic-type ordering of sub-micron-sized domains (Collings, 1990). Growth of such domains may reinforce alignment through growth-induced lipid flow in the direction of alignment. Such flow fields could be established as a result of lipid depletion at the growing ends of the domains. Decreasing the cooling rate increased the size of the domains but did not round the domains, indicating that the equilibrium structure is elongated. The anisotropic nature of the DMTAP domains may indicate that domain growth is correlated along crystallographic directions of the DMTAP two-dimensional lattice. Our observation of increased anisotropy with decreased chain length is exactly the opposite of what is expected if we compare our system to similar monolayer systems. In monolayers, the growth becomes more anisotropic (resulting in, e.g., dendritic growth) as the chain length increases (Weidemann and Vollhardt, 1996). It is believed that this trend occurs because of an increase in crystallinity for longer chains. The short-range charge interactions in our cationic lipid/mica system and its bilayer structure may be involved in the unexpected effects. Alternatively, the second phase transition that we observed in DSC scans may be an important factor in the observed behavior. The two peaks in the DSC scans for DMTAP indicate that when DMTAP is cooled, it enters one gel phase and then another (Silvius, 1991). Upon cooling, domain formation of DMTAP on mica began during the first gel phase. Differences in domain shape between DMTAP and DPTAP may arise, therefore, because the crystallographic order of the first gel phase of DMTAP may be significantly different than the single gel phase observed for DPTAP.

We can compare our results to a recent topographic AFM study of dipalmitoylphosphatidylcholine (DPPC) lipid monolayers in the LE-LC regime that had been transferred to mica. In that case (Hollars and Dunn, 1998), the LE regions appeared to have undergone a condensation process during the transfer that resulted in two different heights of lipid coexisting in micron-scale domains. Such condensation processes have been attributed to the thinning of the water layer between the monolayer and substrate (Fang and Knobler, 1995; Srinivasan et al., 1988). Because the transferred sample in the previous study was readily imaged by contact mode AFM, which generally requires a non-fluid sample, it can probably be assumed that the two coexisting phases were both condensed in nature (at the air-water interface, the LE phase is relatively noncondensed and fluid). A difference in crystalline order and tilt of the transferred lipid would then account for the measured height difference of 0.5 to 0.8 nm between coexisting condensed phases in transferred monolayers. Because our bilayer height differences (~1.4 nm) were approximately twice those of transferred monolayers in the study by Hollars and Dunn (1998) and the chain lengths were similar in both studies, it may be that our bilayers undergo a similar condensation process that results in domain formation. Based on our results, a tilt angle can be easily approximated for the more tilted lipid based on the measured heights of the two lipid phases (~4 nm and 2.6 nm) and the tilt angle of the less tilted lipid. If it can be assumed that the less tilted lipid lies with its acyl chains nearly perpendicular to the monolayer surface, the more tilted lipid is angled approximately 50° from the less tilted lipid.

It can be expected that increasing the headgroup repulsion (by decreasing NaCl concentration) will lower the overall density of the layer. It can also be expected, in the case of two coexisting phases, that lowering the overall density, will increase the relative proportion of the phase of lower density (Möhwald, 1990; Knobler, 1990; Vollhardt et

al., 1993). We observed that increasing headgroup repulsion (by decreasing salt concentration) resulted in an increase in the relative proportion of more tilted phase. This result also indicates that the more tilted phase is of lower density than the less tilted phase. In our system, if the lower density more tilted phase is in larger abundance, it will nucleate and grow into fractal domains surrounded by a continuous network of less tilted lipids. In comparison to Langmuir monolayers, if the lower density LE phase is in larger abundance than the LC phase, it does not form domains of well-defined geometry, since it is a relatively disordered non-crystalline phase. This difference demonstrates that the less dense phase in our study is crystalline in nature.

The propensity for this system to form coexisting lipid phases is even more evident when one looks at bilayers of DPTAP + 3% NBD-PC in 20 mM NaCl that were never heated. In that case, both phases were present, although they are in micron-sized domains. This indicates that cationic lipids deposit at a lower density than the less tilted phase (by analogy, the equivalent of a moderate density monolayer). Very slight mobility and a strong interaction with the substrate may allow condensation into small domains of less tilted lipid; the remaining lipids tilt over into the other preferred phase. Heating of a similarly prepared sample, while remaining below the melting-temperature, resulted in domain growth, presumably because of enhanced mobility.

Other considerations

The NBD-PC probe appears to play a significant role in controlling domain size and shape but not lipid tilt. Whether probe was present or absent in DPTAP samples, we observed the same two step heights of approximately 1.4 nm and 4 nm although the 4 nm step was rare in samples containing probe. Therefore, the probe does not appear to control tilt angle although it does seem to play some role in enhancing surface wetting. Possibly, probe lipids are able to fill defects in the samples. As probe concentration was lowered, domain structure became more filled in and less ramified in appearance and domain size increased indicating that the probe contributed greatly to the unstable growth observed here. In the case of samples formed with no probe, interpretation of domain shape and size was limited by the small scan size (maximum scan size is 100 μm $\times$ 100 μm) possible with AFM. DPTAP samples without probe may have contained domains that were predominantly in the hundreds to thousands of microns in size based on the trend that decreasing probe concentration increases domain size and the size of domains with 2% NBD-PC ($\sim$50 μm). Such large domains would not be detected easily using AFM. Instead, only the flat center (with occasional valleys), edge of a domain, or flat regions between domains (with occasional islands) would be observed.

The differences in domain surface coverage between glass and mica can be qualitatively explained in terms of surface charge. Mica readily undergoes ion exchange in which negative surface sites are occupied by solute ions (Pashley, 1981), including H^+. As a result of the differences in size of ions, the negative surface charge on mica in water is very small, approximately .005 C/m^2, while it is approximately an order of magnitude higher in 20 mM NaCl. The negative surface charge of glass, which does not bind sodium ions strongly (Ong et al., 1992) and therefore should not be significantly affected by NaCl concentration, can be estimated to be approximately 0.1 C/m^2 in weak NaCl solutions or in pure water. This estimate is based on the surface charge of silica, which has been shown to closely approximate the surface charge on glass (Cremer and Boxer, 1999) at pH $\sim$5.5, in which approximately 19% of the OH groups are charged (Ong et al., 1992). Thus, cationic DPTAP bilayers are more condensed on glass in comparison to mica under the same NaCl concentrations because of the relatively larger surface charge of glass.

CONCLUSIONS

Films of cationic lipid (DPTAP and DMTAP) were formed on mica by vesicle fusion. We examined these films in an aqueous environment using both fluorescence microscopy and AFM imaging. AFM images showed that the films were of bilayer thickness and that two preferred bilayer thicknesses coexisted, corresponding to gel phase lipid in a more tilted phase of lipid and a less tilted state. Fluorescence microscopy images revealed that heating and cooling of the deposited bilayers resulted in unstable crystal growth (e.g., fractals) in one or the other phase depending on ionic conditions. In contrast, it is known that domain growth only occurs in the crystalline LC phase in Langmuir monolayers. Therefore, both gel phases here contain a high degree of crystalline order. The fractal shape and rounding of DPTAP domains indicate that domain growth occurred relatively isotropically. However, a shorter chained lipid, DMTAP, displayed anisotropic growth, forming elongated triangle-shaped domains. This result is in contrast to the expected trend of increasing growth disorder with decreasing acyl chain length. Short range charge interactions or the phase behavior of DMTAP (as detected by DSC) in comparison to DPTAP may be important factors in the unexpected behavior seen here. By using DPTAP bilayers on mica and lowering the salt concentration from 20 to 0 mM, the continuous region between domains could be switched from the less tilted to the more tilted phase at approximately 5 mM NaCl; this type of behavior is known as "crossing a percolation threshold". Additionally, the relative abundance of less tilted phase was increased at 20 mM in comparison to 0 mM, demonstrating that ionic screening is an important factor in determining surface density. Taken together, these results suggest that supported bilayers may serve as useful model systems for studying two-dimensional domain growth in lipid bilayers. The surface charge and ionic

strength control the overall surface density (and thus determine the dominant phase) in much the same way as the ionic strength of the subphase or barriers control surface density in Langmuir monolayers. In particular, this system displays unstable domain growth that occurs when domains form very rapidly, for example in rapid cooling of membranes in cell preservation. Additionally, we found that this supported bilayer system displays differences in comparison to Langmuir monolayers, which have often been used to study organic thin film phase behavior and domain formation.

This work was supported in part by the Materials Research Science and Engineering Center Program of the National Science Foundation under award number DMR-9808677. This work was also supported by a Whitaker Foundation biomedical engineering grant. We offer special thanks to Lois and John Crowe, University of California Davis, for use of their differential scanning calorimeter.

REFERENCES

Akamatsu, S., and F. Rondelez. 1992. Two-dimensional pattern formation in langmuir monolayers. *Progr. Colloid Polymer Sci.* 89:209–213.

Barabási, A.-L., and H. E. Stanley. 1995. Fractal concepts in surface growth. Cambridge University Press, Cambridge, UK.

Chernomordik, L., A. Chanturiya, J. Green, and J. Zimmerberg. 1995. The hemifusion intermediate and its conversion to complete fusion: regulation by membrane composition. *Biophys. J.* 69:922–929.

Collings, P. J. 1990. *In* Liquid Crystals: Nature's Delicate Phase of Matter. Princeton University Press, Oxford, UK. Ch. 1.

Cremer, P. S., and S. G. Boxer. 1999. Formation and spreading of lipid bilayers on planar glass supports. *J. Phys. Chem. B.* 103:2554–2559.

Dibble, A. R. G., A. K. Hinderliter, J. J. Sando, and R. L. Biltonen. 1996. Lipid lateral heterogeneity in phosphatidylcholine-phosphatidylserine-diacylglycerol vesicles and its influence on protein kinase C activation. *Biophys. J.* 71:1877–1890.

Fang, Y., and J. Yang. 1997. Two-dimensional condensation of DNA molecules on cationic lipid membranes. *J. Phys. Chem. B.* 101:441–449.

Fang, J., and C. M. Knobler. 1995. Control of density in self-assembled organosilane monolayers by Langmuir-Blodgett deposition. *J. Phys. Chem.* 99:10425–10429.

Hays, L. M., R. E. Feeney, L. M. Crowe, J. H. Crowe, and A. E. Oliver. 1996. Antifreeze glycoproteins inhibit leakage from liposomes during thermotropic phase transitions. *Proc. Natl. Acad. Sci. USA.* 93: 6835–6840.

Hollars, C. W., and R. C. Dunn. 1997. Submicron fluorescence, topology and compliance measurements of phase separated lipid monolayers using tapping-mode near-field scanning optical microscopy. *J. Phys. Chem.* 101:6313–6317.

Hollars, C. W., and R. C. Dunn. 1998. Submicron structure in L-α-dipalmitoylphosphatidylcholine monolayers and bilayers probed with confocal, atomic force, and near-field microscopy. *Biophys. J.* 75: 342–353.

Karlsson, O. P., M. Rytomaa, A. Dahlqvist, P. K. J. Kinnunen, and A. Wieslander. 1996. Correlation between bilayer lipid dynamics and activity of diglucosyldiacylglycerol synthase from *Acholeplasma laidlawii* membranes. *Biochemistry.* 35:10094–10102.

Knobler, C. M. 1990. Seeing phenomena in Flatland: studies of monolayers by fluorescence microscopy. *Science.* 249:870–874.

Korlach, J., P. Schwille, W. W. Webb, and G. W. Feigenson. 1999. Characterization of lipid bilayer phases by confocal microscopy and fluorescence correlation spectroscopy. *Proc. Natl. Acad. Sci. USA.* 96: 8461–8466.

Marsh, D. 1990. Handbook of Lipid Bilayers, CRC Press, Boca Raton, FL.

Masai, J., T. Shibata-Seki, K. Sasaki, H. Murayama, and K. Sano. 1996. Scanning force microscopy characterization of thin lipid films on a substrate. *Thin Solid Films.* 273:289–296.

McKiernan, A. E., R. I. MacDonald, R. C. MacDonald, and D. Axelrod. 1997. Cytoskeletal protein binding kinetics at planar phospholipid membranes. *Biophys. J.* 73:1987–1998.

Möhwald, H. 1990. Phospholipid and phospholipid-protein monolayers at the air/water interface. *Annu Rev. Phys. Chem.* 41:441–476.

Mou, J., D. M. Czajkowsky, Y. Zhang, and Z. Shao. 1995. High-resolution atomic-force microscopy of DNA: the pitch of the double helix. *FEBS Lett.* 371:279–282.

Moy, V. T., D. J. Keller, and H. M. McConnell. 1988. Molecular order in finite two-dimensional crystals of lipid at the air-water interface. *J. Phys. Chem.* 92:5233–5238.

Mukherjee, S., Soe, T. T., and F. R. Maxfield. 1999. Endocytotic sorting of lipid analogues differing solely in the chemistry of their hydrophobic tails. *J. Cell Biol.* 144:1271–1284.

Ong, S., Zhao, X., and K. B. Eisenthal. 1992. Polarization of water molecules at a charged interface: second harmonic studies of the silica/water interface. *Chem. Phys. Lett.* 191:327–335.

Pashley, R. M. 1981. DLVO and hydration forces between mica surfaces in Li^+, Na^+, K^+, and Cs^+ electrolyte solutions: a correlation of double-layer and hydration forces with surface cation exchange properties. *J. Colloid Interface Sci.* 83:531–546.

Rodgers, W. B. C., and J. K. Rose. 1994. Signals determining protein tyrosine kinase and glycosyl-phosphatidylinositol-anchored protein targetting to a glycolipid-enriched membrane fraction. *Mol. Cell. Biol.* 14:5384–5391.

Shenoy-Scaria, A. M., D. J. Dietzen, J. Kwong, D. C. Link, and D. M. Lublin. 1994. Cysteine-3 of Src family protein tyrosine kinases determines palmitoylation and localization in Caveolae. *J. Cell Biol.* 126: 353–363.

Sikes, H. D., Woodward, I. V., J. T., and D. K. Schwartz. 1996. Pattern formation in a substrate-induced phase transition during Langmuir-Blodgett transfer. *J. Phys. Chem.* 100:9093–9097.

Sikes, H. D., and D. K. Schwartz. 1997. A temperature-dependent two-dimensional condensation transition during Langmuir-Blodgett deposition. *Langmuir.* 13:4704–4709.

Silvius, J. R. 1991. Anomalous mixing of zwitterionic and anionic phospholipids with double-chain cationic amphiphiles in lipid bilayers. *Biochim. Biophys. Acta.* 1070:51–59.

Srinivasan, M. P., B. G. Higgins, and P. Stroeve. 1988. Entrainment of aqueous subphase in Langmuir-Blodgett films. *Thin Solid Films.* 159: 191–205.

Tamm, L. K., C. Bohm, J. Yang, Z. Shao, J. Hwang, M. Ediden, and B. Betzig. 1996. Nanostructure of supported phospholipid monolayers and bilayers by scanning probe microscopy. *Thin Solid Films.* 284:813–816.

Trevors, J. T. 1997. Molecular evolution in bacteria: surfaces, cathodes and anodes. *Antonie van Leeuwenhoek.* 71:363–368.

Vaz, W. L. C. 1995. Percolation properties of two-component, two-phase phospholipid bilayers. *Mol. Membr. Biol.* 12:39–43.

Verkade, P., and K. Simons. 1997. Lipid microdomains and membrane trafficking in mammalian cells. *Histochem. Cell Biol.* 108:211–220.

Vollhardt, D., U. Gehlert, and S. Siegel. 1993. Temperature-dependent studies of the phase behavior of 1-monostearoyl-rac-glycerol monolayers. *Coll. Surf. A.* 76:187–195.

Weidemann, G., and D. Vollhardt. 1995. Long-range tilt order in phospholipid monolayers: the inner structure of dimyristoyl-phosphatidylethanolamine domains. *Thin Solid Films.* 264:94–103.

Weidemann, G., and D. Vollhardt. 1996. Long-range tilt orientation in phospholipid monolayers: a comparative study. *Biophys. J.* 70: 2758–2766.

Yang, X. M., D. Xiao, Z. H. Lu, and Y. Wei. 1994a. Observation of chiral domain morphology in a phospholipid Langmuir-Blodgett monolayer by atomic force microscopy. *Phys. Lett. A.* 193:195–198.

Yang, X. M., D. Xiao, S. J. Xiao, and Y. Wei. 1994b. Domain structures of phospholipid monolayer Langmuir-Blodgett films determined by atomic force microscopy. *Appl. Phys. A.* 59:139–143.